IN-73
65103
P-44

NASA Contractor Report 4054

Statistical Analysis of Secondary Particle Distributions in Relativistic Nucleus-Nucleus Collisions

Stephen C. McGuire

GRANT NAG8-027
MARCH 1987

NASA

NASA Contractor Report 4054

Statistical Analysis of Secondary Particle Distributions in Relativistic Nucleus-Nucleus Collisions

Stephen C. McGuire
Alabama A&M University
Normal, Alabama

Prepared for
George C. Marshall Space Flight Center
under Grant NAG8-027

National Aeronautics
and Space Administration

Scientific and Technical
Information Branch

1987

ACKNOWLEDGEMENTS

The author expresses his appreciation to T. A. Parnell, Y. Takahashi, and M. Weisskopf for many helpful discussions of this work and to B. H. Peterson, F. E. Roberts, and J. Watts for assistance with the computations. This research was sponsored by the National Aeronautics and Space Administration via Grant No. NAG8-027. The data and the results of the analysis presented in this paper form part of the work of the JACEE collaboration:

T. H. Burnett, S. Dake, M. Fuki, J. C. Gregory, T. Hayashi, R. Holynski, J. Iwai, W. V. Jones, A. Jurak, J. J. Lord, O. Miyamura, T. Ogata, T. A. Parnell, T. Saito, S. Strausz, T. Tabuki, Y. Takahashi, T. Tominaga, B. Wilczynska, R. J. Wilkes, W. Wolter, and B. Wosiek.

TABLE OF CONTENTS

LIST OF ILLUSTRATIONS

LIST OF TABLES

I. INTRODUCTION

Presently there is much interest in relativistic nucleus-nucleus collisions because of the prediction by quantum chromodynamics(QCD) that under conditions of sufficiently high energy density a new state of nuclear matter, the quark gluon plasma(QGP), can be formed[1]. The plasma may be observed in real time by detecting weakly interacting particles such as photons or lepton pairs that emanate from the plasma. Alternatively, it is possible to search for a characteristic signal in the angular distributions of secondary particles emitted in the collision. The latter approach is the only one that can be used when the secondary particles are observed in passive detectors such as balloon-borne emulsion chambers[2].

Recent data from accelerator-based heavy ion experiments indicate that compressional nuclear forces are observable in nucleus-nucleus collisions at high energy[3,4]. During the collision nuclear matter is assumed to behave like a fluid whose motion is governed by the equations of hydrodynamics. Some fraction of the incident kinetic energy is transformed into potential or compressional energy. The fact that the nuclear matter is made up of neutrons and protons is ignored except in the final stages of the collision when the matter has expanded and cooled. A fraction of the particles emitted in the collision may emerge moving in a preferred direction[5,6] allowing for the observation of the "footprint" of the QGP production in the angular distribution of the secondary particles.

In this paper we report on the application of statistical analyses to the angular distributions of secondary particles emitted in relativistic nucleus-nucleus collisions. In particular, we have examined a set of JACEE-3 events for the presence of correlations in the azimuthal distributions of the secondary particles. Two approaches have been used here. In the first case, we test for asymmetry in the entire data set of events using the method of composite unit vectors[7-9]. Secondly, chisquare goodness-of-fit tests and discrete Fourier transform analysis are used to examine event-by-event for correlations between particle intensity and azimuthal angle. Our analysis is further extended to include searches for evidences of non-statistical fluctuations in the pseudorapidity distributions of single events. It is expected that the investigation of non-statistical fluctuations in single events will be most productive for high multiplicity collisions since it is assumed that nucleus-nucleus collisions are made up of many incoherent elementary processes[10-12].

II. METHOD OF COMPOSITE UNIT VECTORS

The method of composite unit vectors permits one to test for azimuthal asymmetry in the distribution of an entire data set of events. A summary of the reactions included in this set and the range of energies covered is provided in Table I. In the method, the direction of the emitted particle is projected onto the azimuthal plane and a unit vector, $\hat{r}_i$, is constructed from this projection. As shown in figure 1., $\vec{R}_i$ describes the emitted particle's direction and $R_i SIN\emptyset_i$ is the magnitude of its projection onto the azimuthal plane. The unit vector in the azimuthal plane simply becomes

$$\hat{r}_i = (COS\emptyset_i)\ \hat{i} + (SIN\emptyset_i)\ \hat{j} \quad . \qquad (1)$$

For each event we construct a quantity, w, given by

$$w = \frac{\left| \sum_i \hat{r}_i \right|^2}{n} \qquad i = 1,n \quad , \qquad (2)$$

where n is the number of secondaries and $\emptyset_i$ is the azimuthal angle associated with the ith emitted particle. We note that events with a small degree of asymmetry will have w values near or equal to zero and that w will increase with increasing asymmetry. If it is assumed that the emitted particles are randomly distributed in the angle $\emptyset$, the situation is mathematically equivalent to the problem of calculating the probability distribution associated with n frequencies of unit amplitude each possessing a random phase. The

Table I. Summary of reactions treated in this work. [a]The energy for at least one event in this group was not available at the time of this analysis.

REACTION	RANGE OF MULTIPLICITIES	ENERGY RANGE (GeV/nucleon)
N_i ---> C	28	56
Fe ---> Pb	21 - 165	28 - 48[a]
Fe ---> Ag	26 - 69	25 - 52[a]
Fe ---> O	11 - 132	25 - 55
Fe ---> C	8 - 105	22 - 51[a]
Fe ---> N	12	28
Cr ---> Pb	65 - 94	25 - 48
Cr ---> C	23 - 113	23 - 45
V ---> O	14	27
Ti ---> AgBr	20 - 283	24 - 41
Ti ---> O	15	26
Ti ---> C	6 - 39	32 - 61[a]
Ca ---> Ag	108	61
Ca ---> C	16	35
Ar ---> Pb	5	25
Ar ---> C	25	61
S ---> C	21	35
He ---> Ag	20	55
He ---> C	9 - 59	61

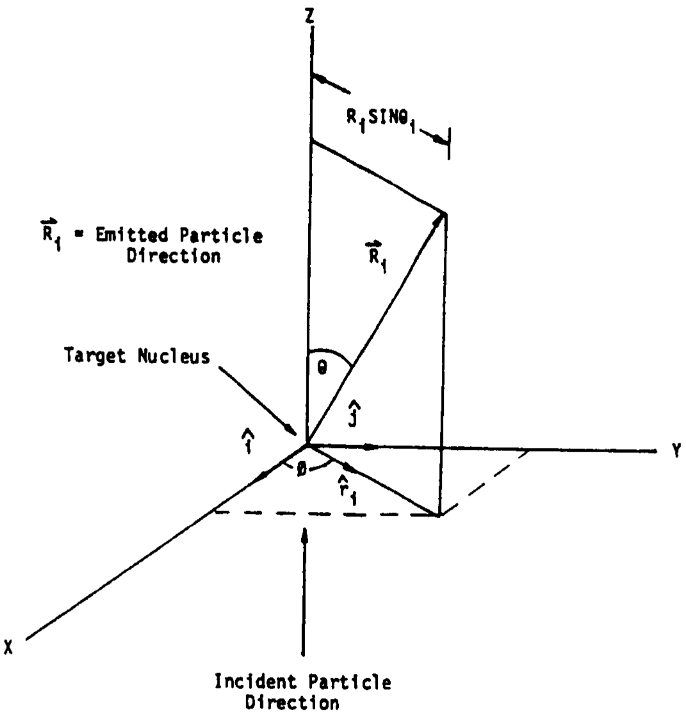

Figure 1. Coordinate system diagram illustrating the composite unit vector method.

resulting probability distribution, when expressed in terms of the parameter w, is approximated by the exponential form[13],

$$P(w)dw \sim \exp(-w)dw. \qquad (3)$$

It therefore should be possible to obtain a measure of the azimuthal asymmetry in the entire data set by constructing the distribution of events in w and comparing its shape to the exponential. Deviation from this exponential behavior may then be interpreted as an indication of anisotropy in the data.

The distribution in w for the JACEE-3 events analyzed is shown in figure 2. The solid curve in the plot is the renormalized exponential function. The dashed line is the result of of a least squares fit to a single exponential,

$$n = A\exp(-Bw) \quad , \qquad (4)$$

where $A = 24.5694$ and $B = 0.84962$. In general, the agreement between the experimental distribution and the theoretical curves is good. This result is not unusual in that purely statistical fluctuations that occur event to event will be lost when averaging over a sufficiently large set events. It is therefore important that single events be investigated for evidences of non-statistical fluctuation. In the next section of this report we present a method for the analysis of structure observed in the azimuthal distributions of single events.

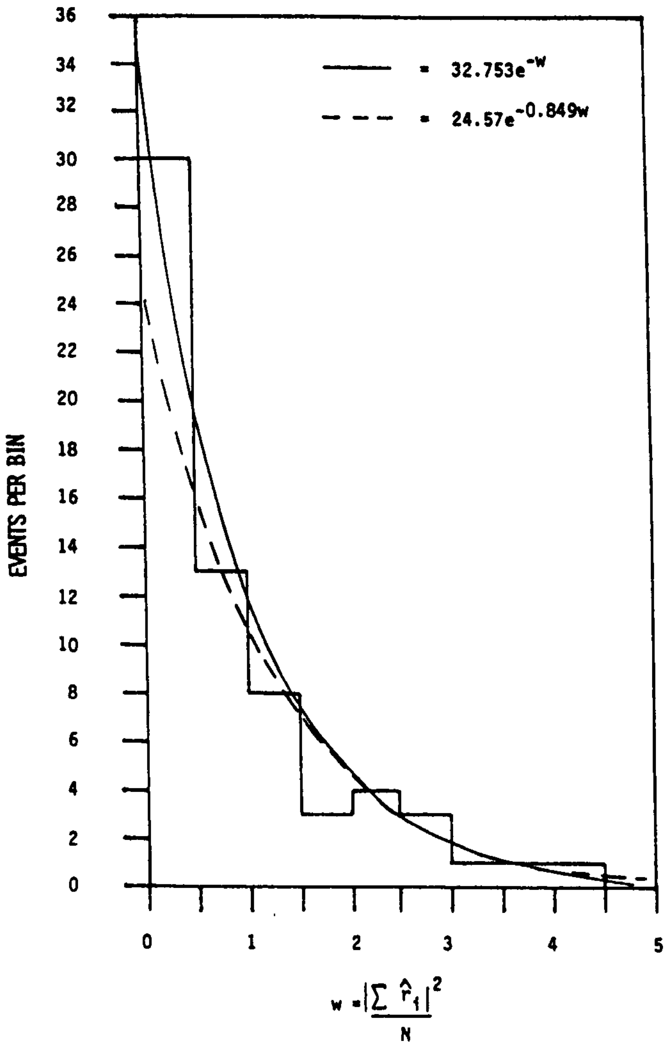

Figure 2. Asymmetry distribution plot for the 63 JACEE-3 events.

III. SINGLE EVENT ANALYSIS

A. Chisquare Tests

In order to examine more closely the question of nonuniformity in the azimuthal angular distributions, each distribution was subjected to a null hypothesis test wherein the probability that its intensity pattern could be attributed to chance occurrence was determined. In effect, a least squares fit of the data to the average of the distribution was performed and a chisquare value given by

$$\chi^2 = \sum_i \left[\frac{(N_i - \overline{N})^2}{\sigma_i^2}\right] \qquad i = 1, N_b \qquad (5)$$

was evaluated for each event[14]. In the present case χ^2 corresponds to the sum of the squares of the residuals with each residual weighted by its fractional standard deviation. The integral chisquare probability[15], P_χ, was also determined for each event. It represents the probability that a randomly chosen set of N data points will yield a value of χ^2 as large as or larger when compared with the parent distribution. An assumption that is inherent to this part of the analysis is that the experimental χ^2 values are characterized by a chisquare distribution of degrees of freedom. This will indeed be the case if the χ_i's are independent and identically distributed variables each following a normal distribution with a mean of zero and unit variance. The exercise of evaluating this assumption is complicated by the relatively small number of events in the sample and the fact that the events generally correspond to different reactions rather than a collection of events from the same reaction. Further, variations in the multiplicity among events lead to variations in the values associated with the individual angular distributions. Thus, the events that fall within a given bin of the experimental χ^2 distribution will in general have a range of values. With these considerations in mind we have taken the following approach to obtaining a comparison between theory and experiment.

The general form of the chisquare distribution is given by

$$P(\chi^2;\nu) = \frac{(\chi^2)^{(\nu-2)/2}\exp(-\chi^2/2)}{(2)^{\nu/2}\,\Gamma(\nu/2)}, \qquad (6)$$

where ν is the number of degrees of freedom associated with the distribution. For each bin in the experimental χ^2 distribution we construct an average probability given by

$$\overline{P}_k = \frac{\displaystyle\sum_{i=1}^{N} \frac{(\chi_i^2)^{(\nu_i-2)/2}\exp(-\chi_i^2/2)}{(2)^{\nu_i/2}\,\Gamma(\nu_i/2)}}{N}, \qquad (7)$$

where

N = number of χ_i^2 values that fall within the kth bin,

k = index specifying the bin,

χ_i^2 = chisquare value obtained for the ith angular distribution

and

ν_i = number of degrees of freedom for the ith angular distribution.

The $\overline{P}_k$ values are normalized to satisfy the criterion,

$$\sum_{k=1}^{N_b} \overline{P}_k = N_E \ . \tag{8}$$

N_b is the number of bins in the experimental χ_i^2 distribution and N_E is the total number of events in the data set. The comparison between the above theory and the experiment is provided in figure 3. The shape of the two distributions is seen to be in good qualitative agreement thereby supporting the assumption upon which the integral probabilities are based.

B. Discrete Fourier Transform Analysis of Azimuthal Distributions

Three events with relatively high statistics were chosen for discrete Fourier transform (DFT) analysis[16,17]. The events are identified in Table II, and their distributions are shown in figures 4a-4c and 5a-5c. It should be noted that the number of bins in set 4 is based on an optimization of the sensitivity of the null hypothesis test. The criterion for the Fourier analysis is that the number of bins be an integral power of two. The exact discrete transform was determined for each distribution according to the relationship

$$N_i = N_{av} + \sum_{k=1}^{N_b/2} A_k[\mathrm{COS}(k\omega t_i + /0_k)] \ , \tag{9}$$

where N_b = number of bins in the distribution,

N_{av} = average number of particles per bin,

k = index over which the sum is performed,

A_k = calculated Fourier amplitudes,

$\emptyset_k$ = calculated Fourier phases, and

N_i = predicted value of the number of counts in the bin.

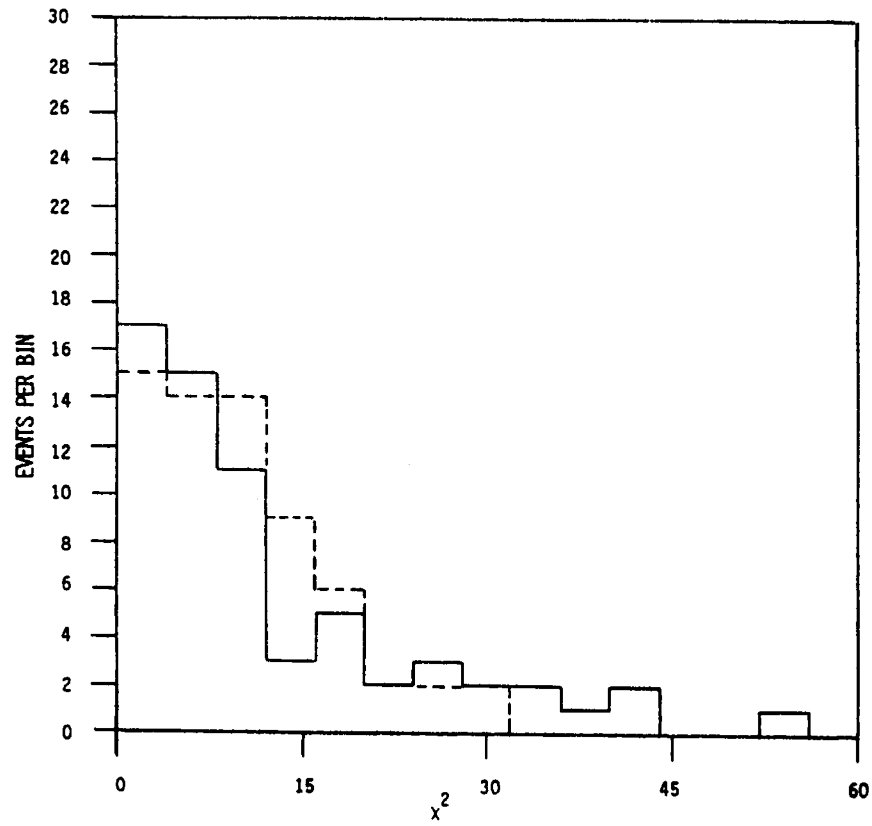

Figure 3. Comparison of experimental and theoretical χ^2 distributions in this work. The solid line is the data and the dashed line is the result of the calculation based on equations (7) and (8).

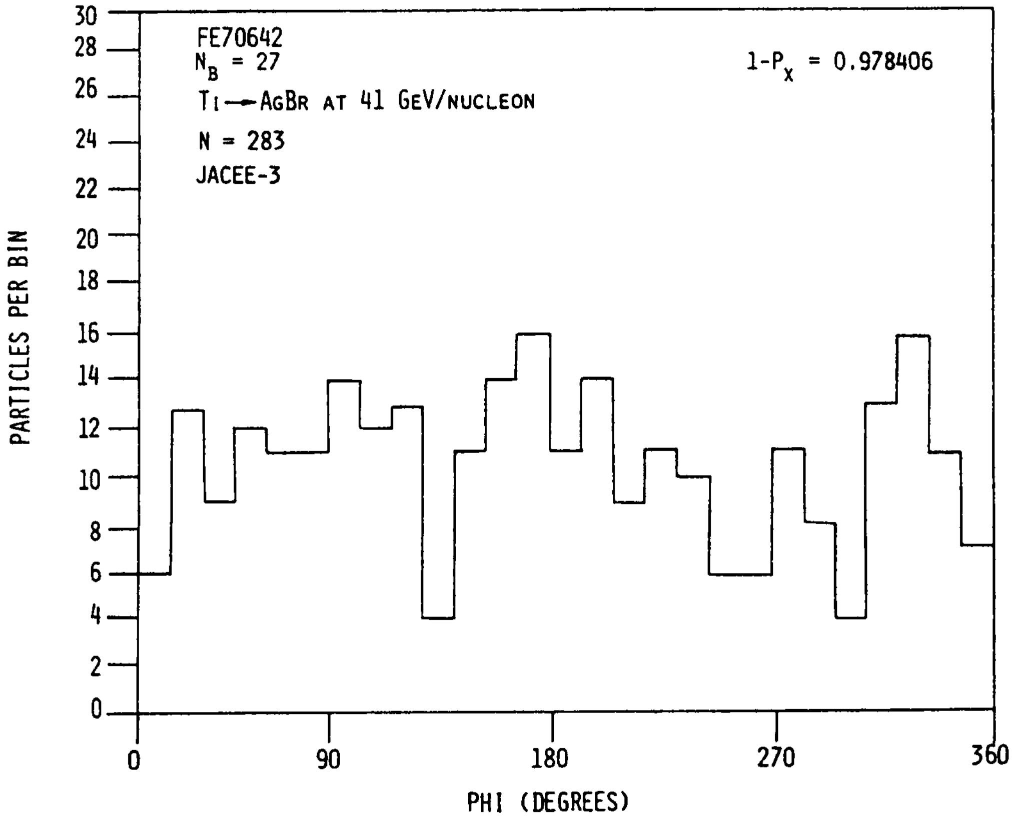

Figure 4a. Azimuthal distribution of emitted particles for event FE70642, Ti $\longrightarrow$ AgBr at 41 GeV/nucleon. $(1 - P_X) = 0.978406$.

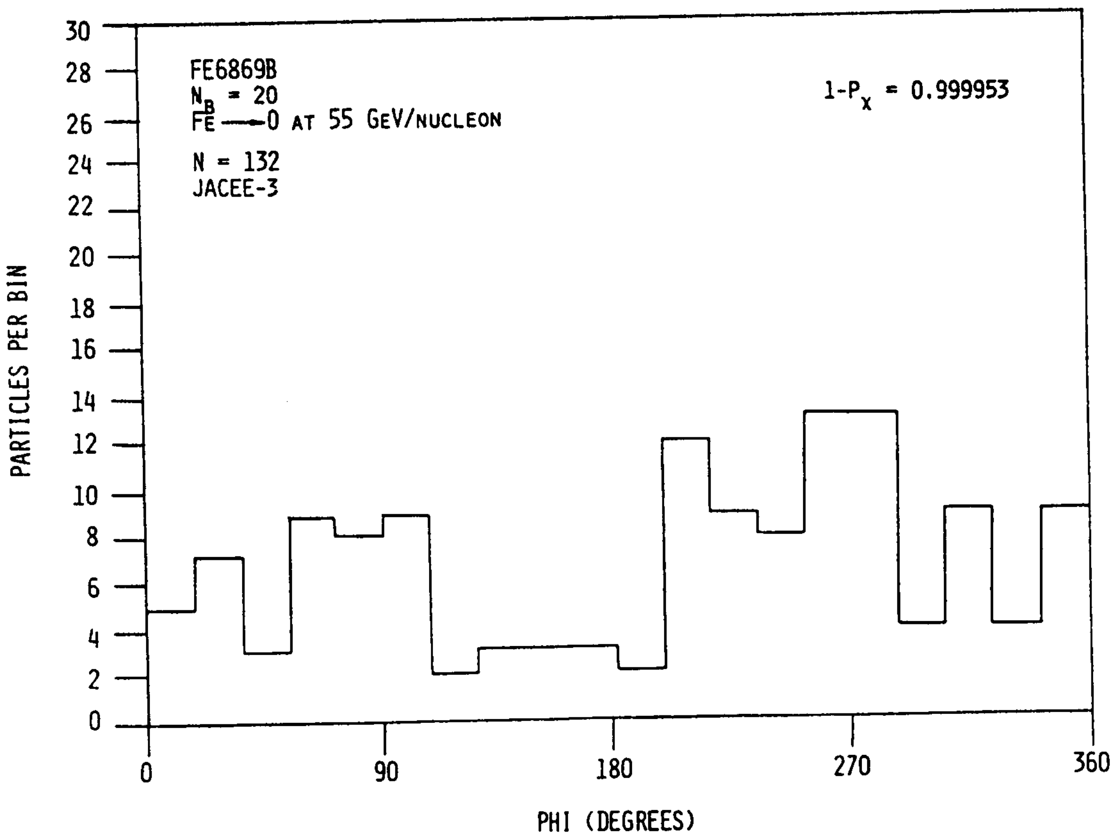

Figure 4b. Azimuthal distribution of emitted particles for event FE6869B, Fe → O at 55 GeV/nucleon. $(1 - P_{\chi}) = 0.999953$.

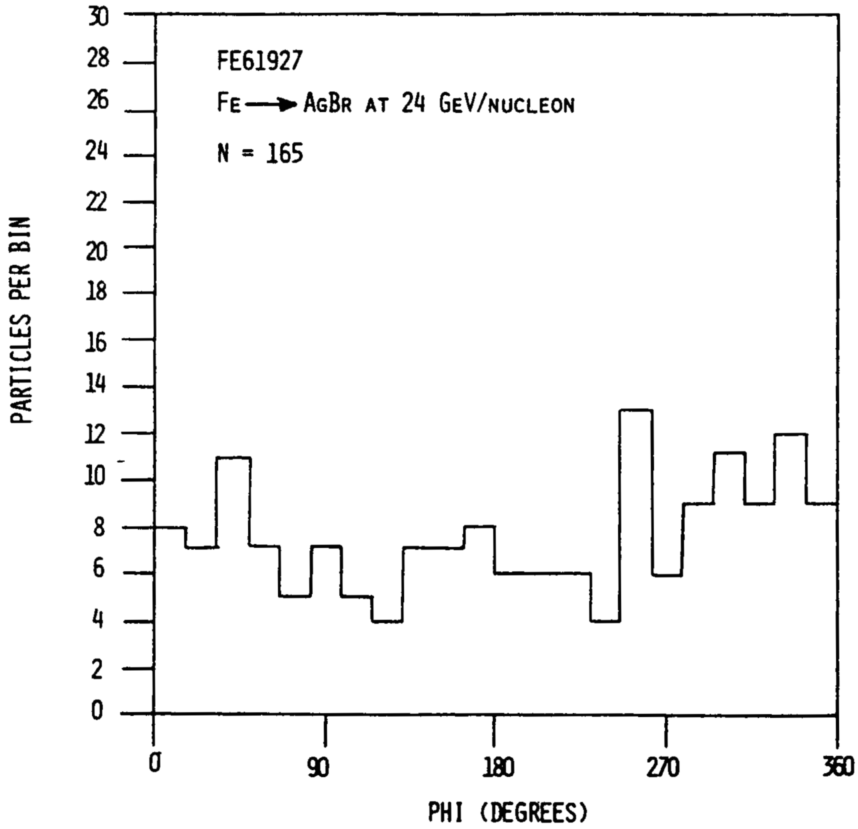

Figure 4c. Azimuthal distribution of emitted particles for event FE61927, Fe ⟶ AgBr at 24 GeV/nucleon. $(1 - P_\chi) = 0.29763$.

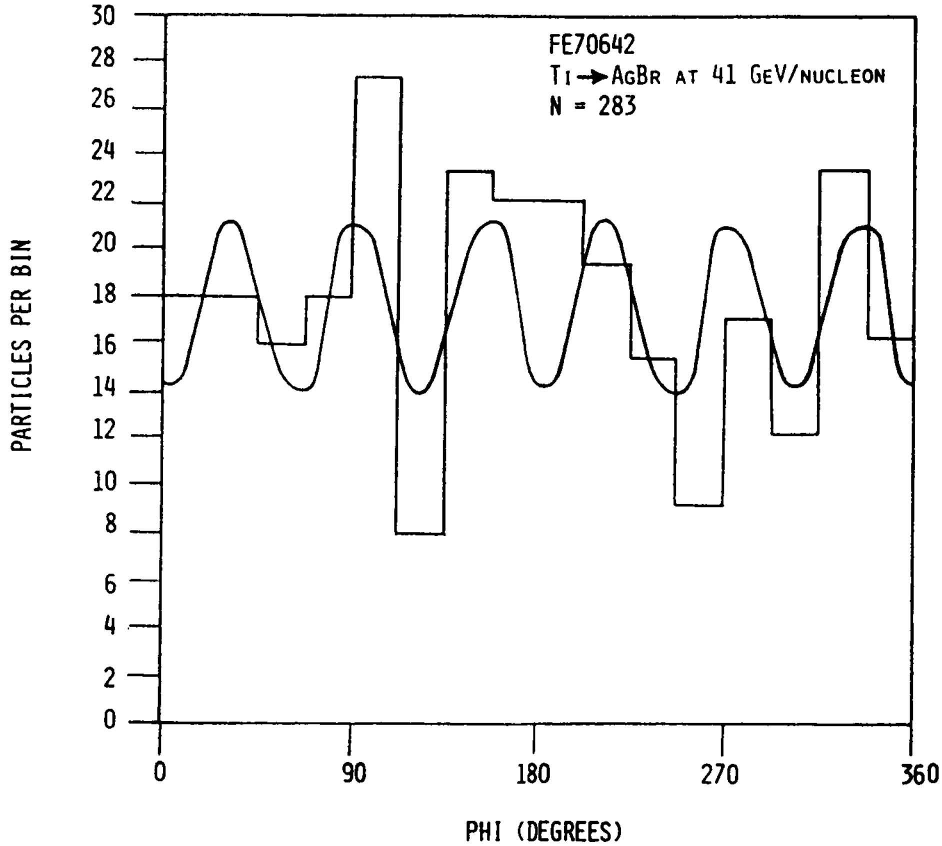

Figure 5a. Azimuthal distribution for event FE70642. The solid curve drawn through the points is the principal component of the fourier transform and corresponds to the function $N_i = N_{av} + A_6 COS(6\,\omega t_i + \emptyset_6)$.

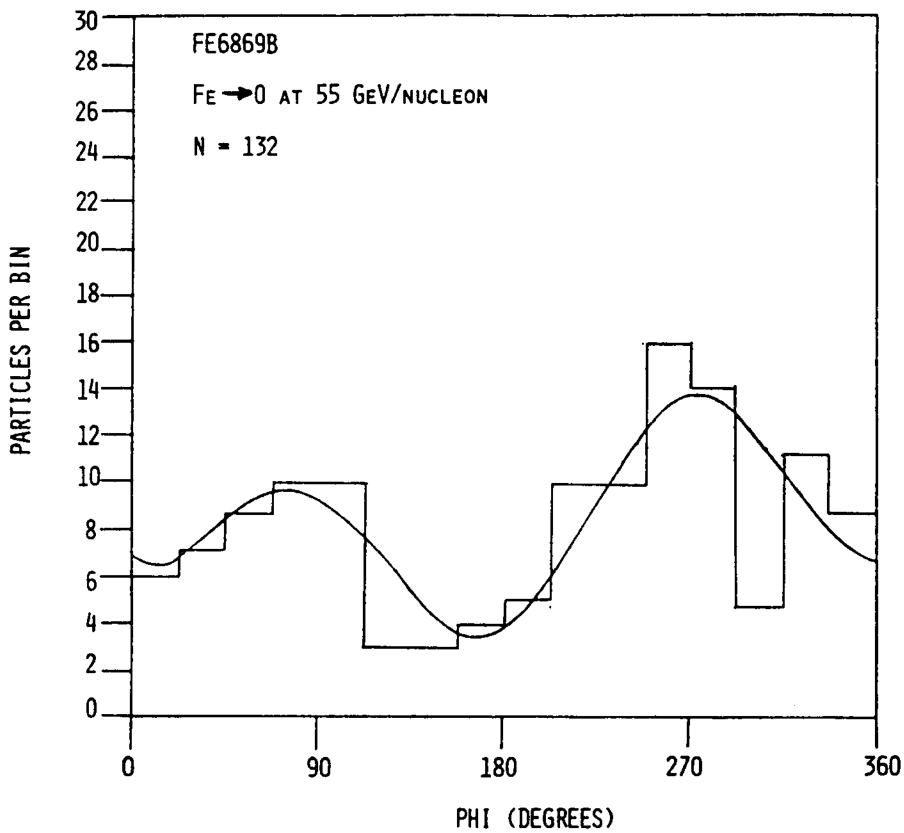

Figure 5b. Azimuthal distribution for event FE6869B. The solid curve drawn through the points corresponds to the function $N_i = N_{av} + A_1 \cos(\omega t_i + \emptyset_1) + A_2 \cos(2\omega t_i + \emptyset_2)$.

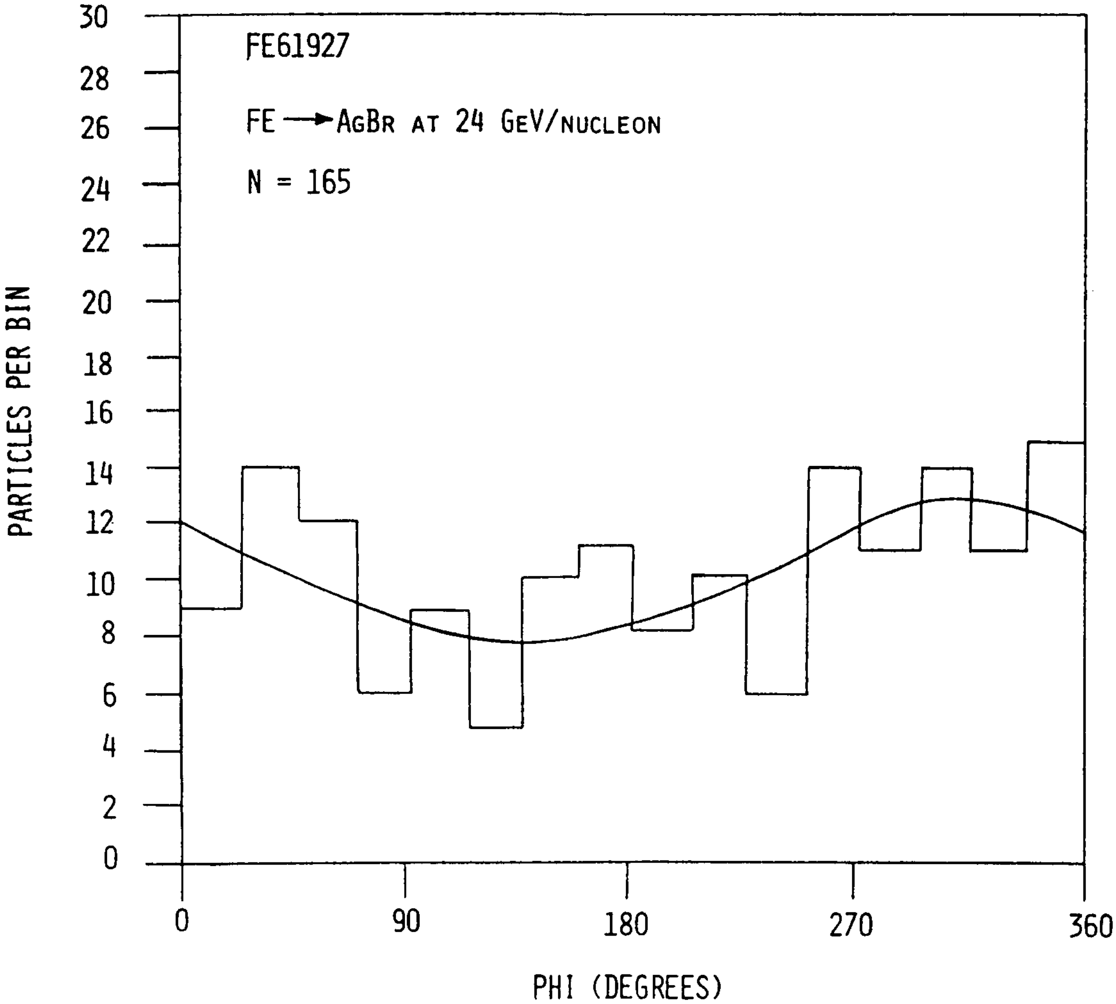

Figure 5c. Azimuthal distribution for event FE61927. The solid curve drawn through the points corresponds to the function $N_i = N_{av} + A_1 \cos(\omega t_i + \emptyset_1)$.

Table II. Reactions for which discrete Fourier transform analysis was performed on the azimuthal angular distribution.

EVENT	REACTION	ENERGY (GeV/nucleon)	N	$(1-P_{\chi})_{exp}$
FE70642	Ti ---> AgBr	41	283	0.978406
FE6869B	Fe ---> O	55	132	0.999953
FE61927	Fe ---> AgBr	24	165	0.297630

The quantity ωt_i is the angle at which the N_i are calculated. The complete results of the Fourier analysis are given in Appendix A. Although eight Fourier amplitudes were calculated by the procedure, each is not necessarily of equal importance to the reconstruction of the original distribution. In order to judge the relative importance of a given amplitude, an integral chisquare probability, P_{χ}, has been calculated for each. The P_{χ} is given by

$$P_{\chi}(\chi_k^2;\ \nu) = \int_0^{\chi_k^2} \frac{(\chi^2)^{(\nu-2)/2} \exp(-\chi^2/2) d\chi^2}{(2)^{\nu/2}\ \Gamma(\nu/2)}, \tag{10}$$

where

$$\chi_k^2 = \sum_{i=1}^{N_b} \left[\frac{(N_i - N_{ik})^2}{\sigma_i^2}\right], \tag{11}$$

and k refers to a single amplitude in equation (9). According to equation (10) large values of P indicate a poor fit and small values indicate a good fit. This approach permits one to easily determine whether the character of a given distribution is dominated by a subset of amplitudes. With this idea in mind, the solid curves shown in figures 5a-5c were drawn to show those amplitudes that have the smallest probabilities of chance occurrence. Of the three events, FE6869B appears to be the only one well characterized by two slowly varying components[18]. The distribution for event FE70642 on the other hand is best characterized by a rapidly varying amplitude which is more typical of noise.

C. Fluctuation Analysis of the Pseudorapidity Distributions

We have used the method of Takagi[19] to test for nonstatistical fluctuations in the pseudorapidity distributions of individual events. This method involves several steps that are only summarized here. First, a smooth function, $f_s(\eta)$ that reflects the average properties of the distribution is determined by least squares fit of the experimental distribution to a superposition of Chebyshef polynomials[20]. The number of terms in the sum is governed by the expansion that minimizes the chisquare value for the fit. Thus, we make the definition

$$f_s(\eta) = a_o/2 + \sum_{k=1}^{m} a_k T_k(z) \equiv f_s^m(\eta). \qquad (12)$$

If there are L bins in the histogram of the distribution, $m < L-1$ and $z = (2\eta-\eta_{min} - \eta_{max})/(\eta_{max} - \eta_{min})$. $T_k(z)$ is the Chebyshef polynomial of degree k and $f(\eta)$ is known for the range $\eta_{max} \geq \eta \geq \eta_{min}$. The total vertical length, V, of the experimental histogram is then used as a measure of the fluctuations in the distribution, i.e.,

$$V_{exp} = \sum_{i=1}^{L+1} |f(\eta_i) - f(\eta_{i-1})| \tag{13}$$

where $f(\eta_o) = f(\eta_{L+1}) \equiv 0$. The pseudorapidity distribution is then simulated by a Monte Carlo procedure. In the present case the method of Von Neumann rejection[21] was used to produce the pseudorapidity distributions for many "equivalent" events. For each simulation, the number of secondary particles was held fixed to the experimentally observed value. Points within the range $\eta_{max} \geq \eta \geq \eta_{min}$ were sampled according to $f_s(\eta)$. The Monte Carlo data obtained should contain distributions of purely statistical fluctuations that can be compared with the fluctuations in the real events.

Two examples of smooth fits, $f_s(\eta)$, are provided in figures 6 and 7 together with their empirical distributions. For comparison, the distributions resulting from single event simulations are shown in figures 8a and 8b for events FE6869B and FE70642, respectively. As expected, distributions based on the average of 250 event simulations reflect the features of the empirical fits for these events. The plots are provided in figures 9a and 9b. Note further from figures 10 and 11 that the experimental fluctuation values, V_{exp}, fall well within the simulated V distributions thus indicating that the fluctuations in the empirical data are largely, if not purely, statistical in nature.

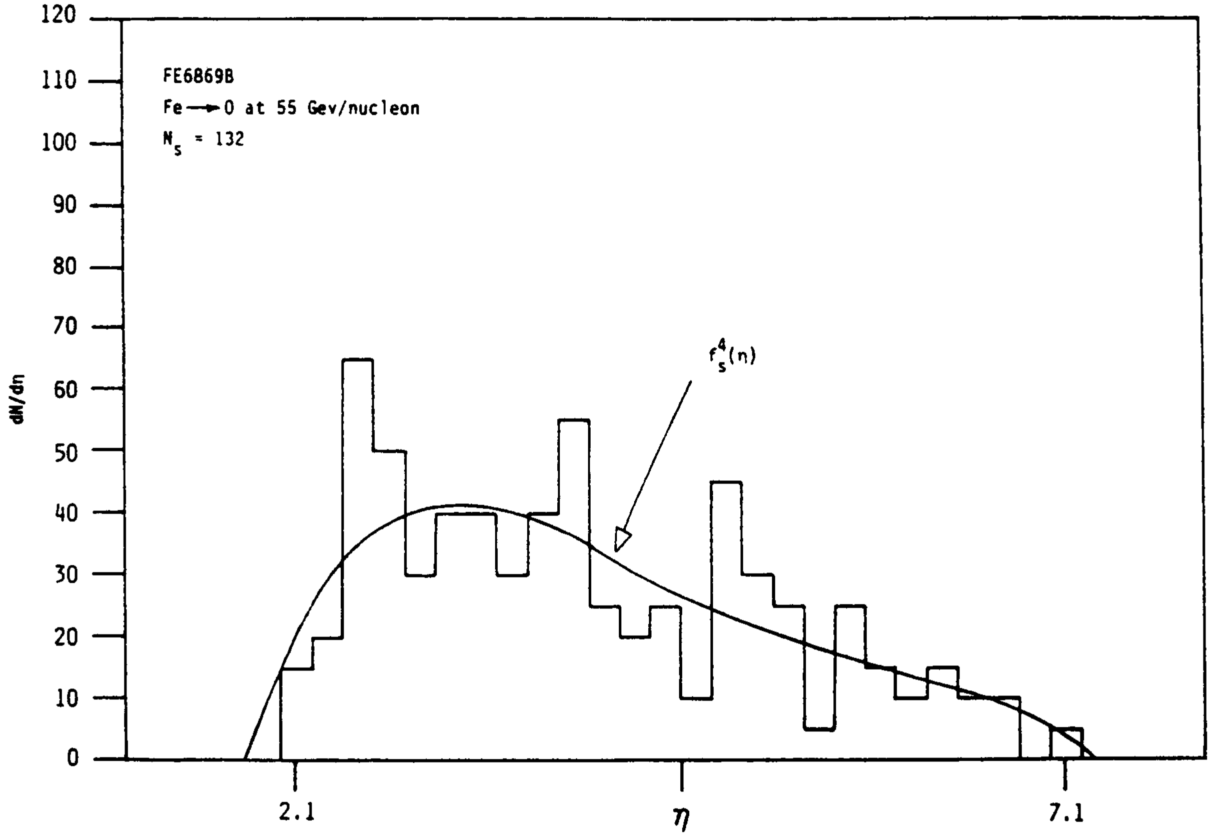

Figure 6. Experimental pseudorapidity distribution for event FE6869B. The solid curve is the result of a least squares fit of the data to the function:

$$f_s^4\,(\eta) = a_0/2 + \sum_{k=1}^{4} a_k\, T_k\,(z).$$

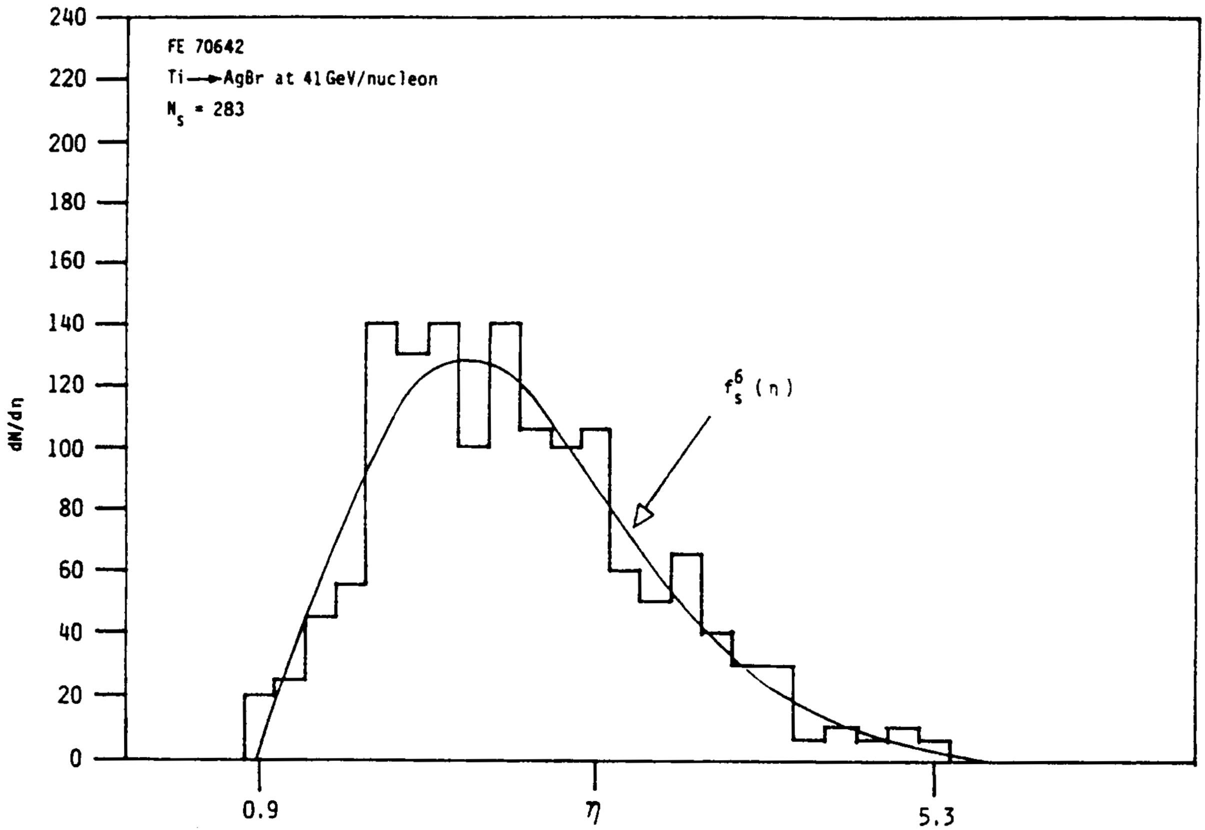

Figure 7. Experimental pseudorapidity distribution for event FE70642. The solid curve is the result of a least squares fit of the data to the function:

$$f_s^6\,(\eta) = a_0/2 + \sum_{k=1}^{6} a_k\, T_k\,(z).$$

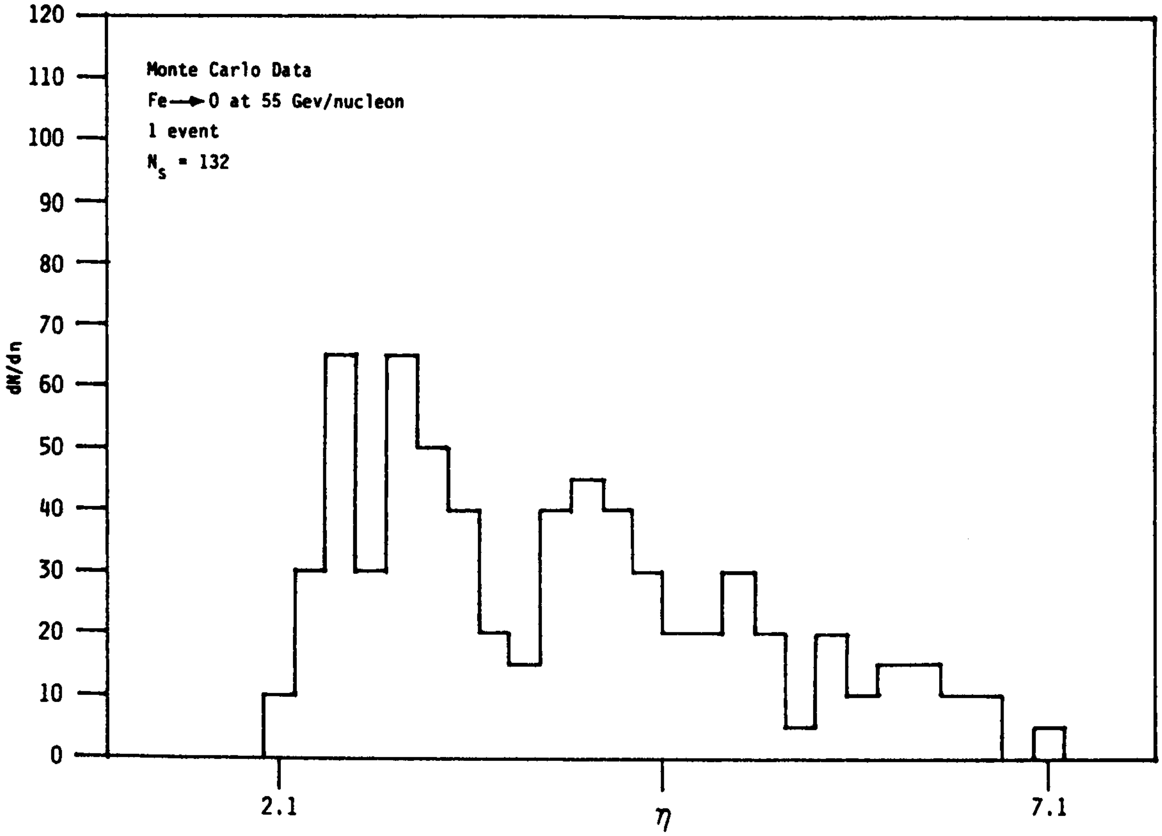

Figure 8a. Single event simulation of the distribution function, f_s^4 (η), for event FE6869B.

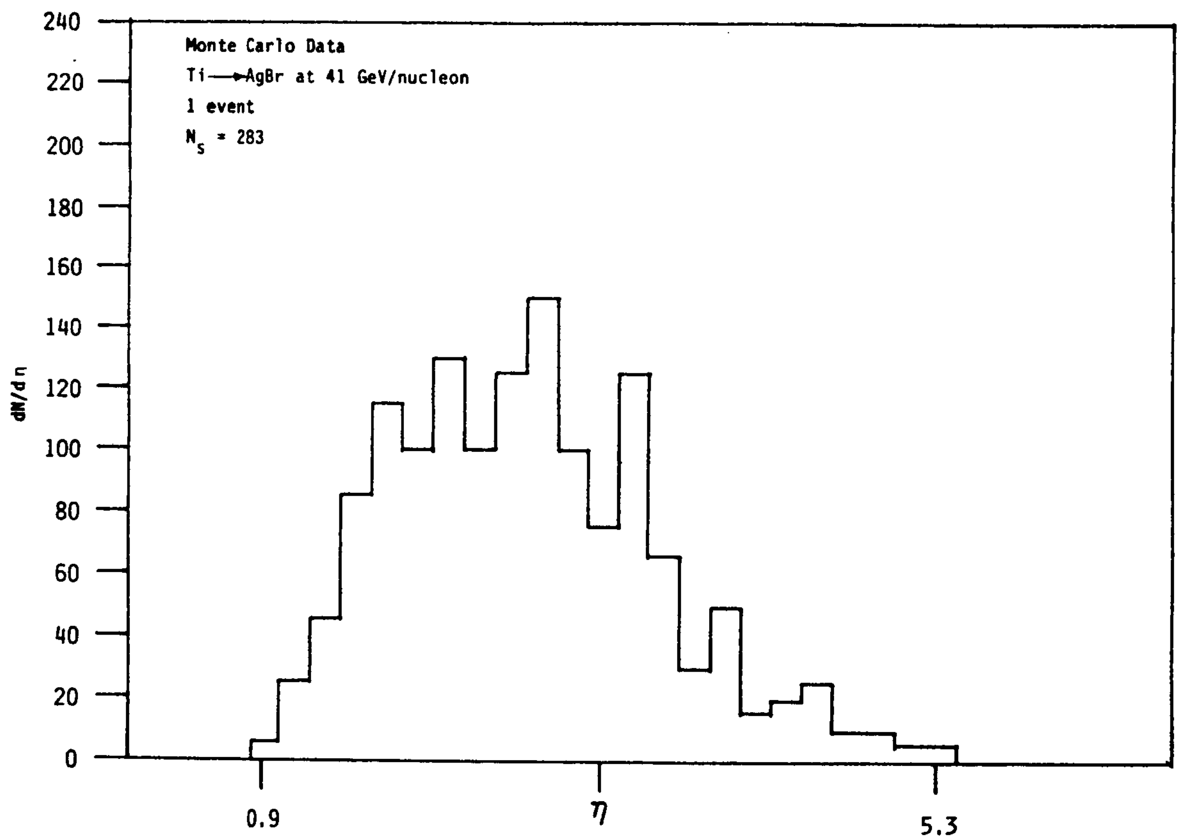

Figure 8b. Single event simulation of the distribution function, $f_s^6(\eta)$, for event FE70642.

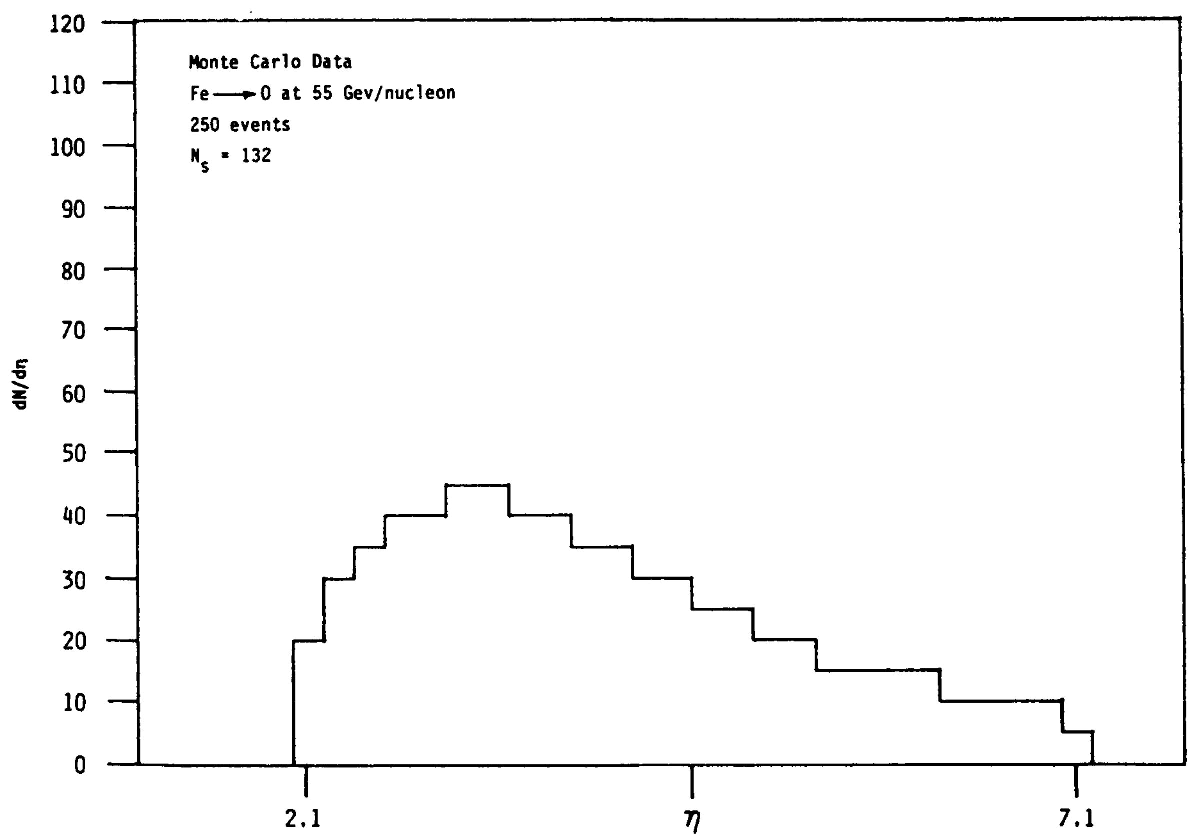

Figure 9a. This plot shows the average distribution resulting from a 250 event simulation of the function, f_s^4 (η), for event FE6869B.

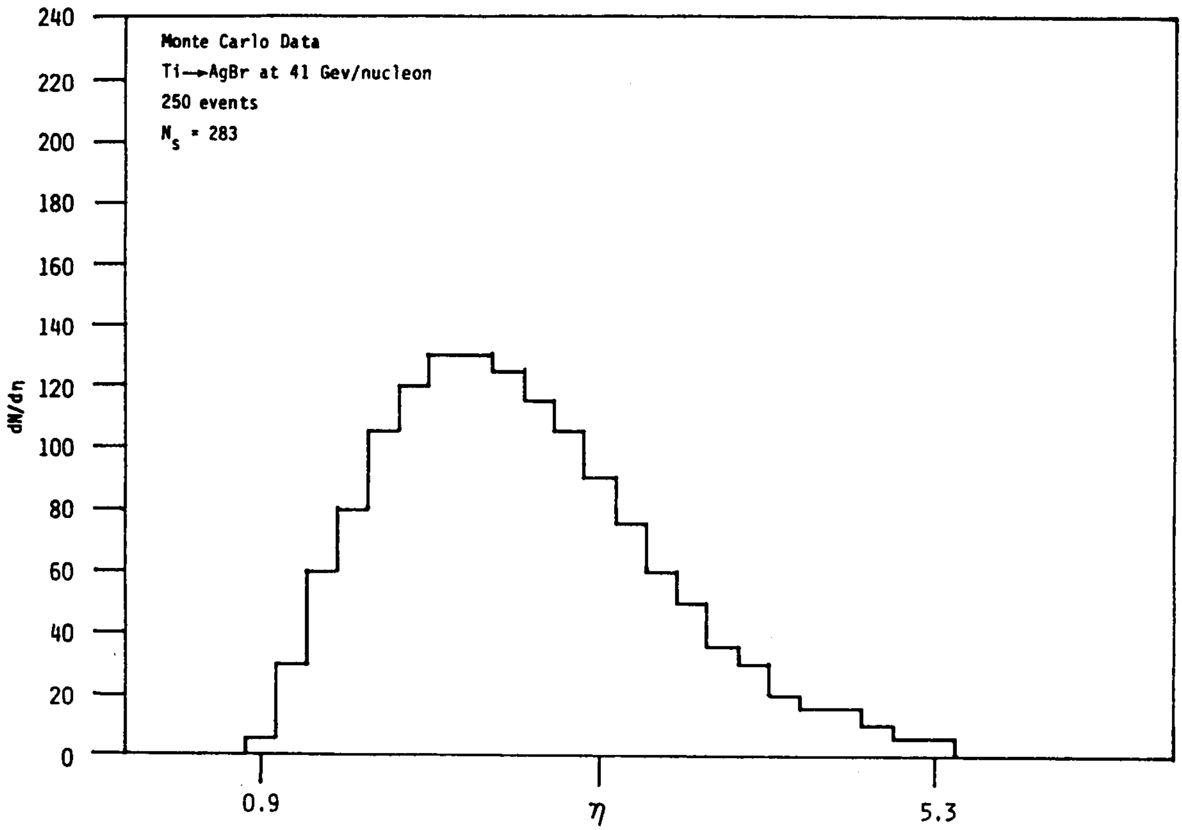

Figure 9b. This plot shows the average distribution resulting from a 250 event simulation of the function, $f_s^6(\eta)$, for event FE70642.

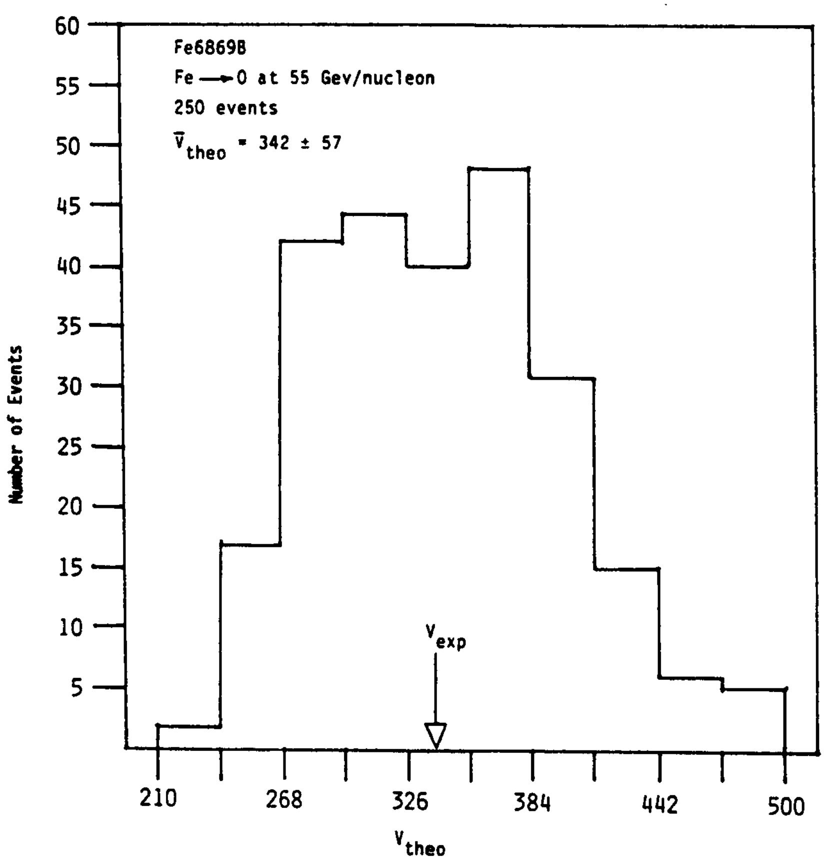

Figure 10. Distribution of the theoretical fluctuations, V_{theo}, for event FE6869B.

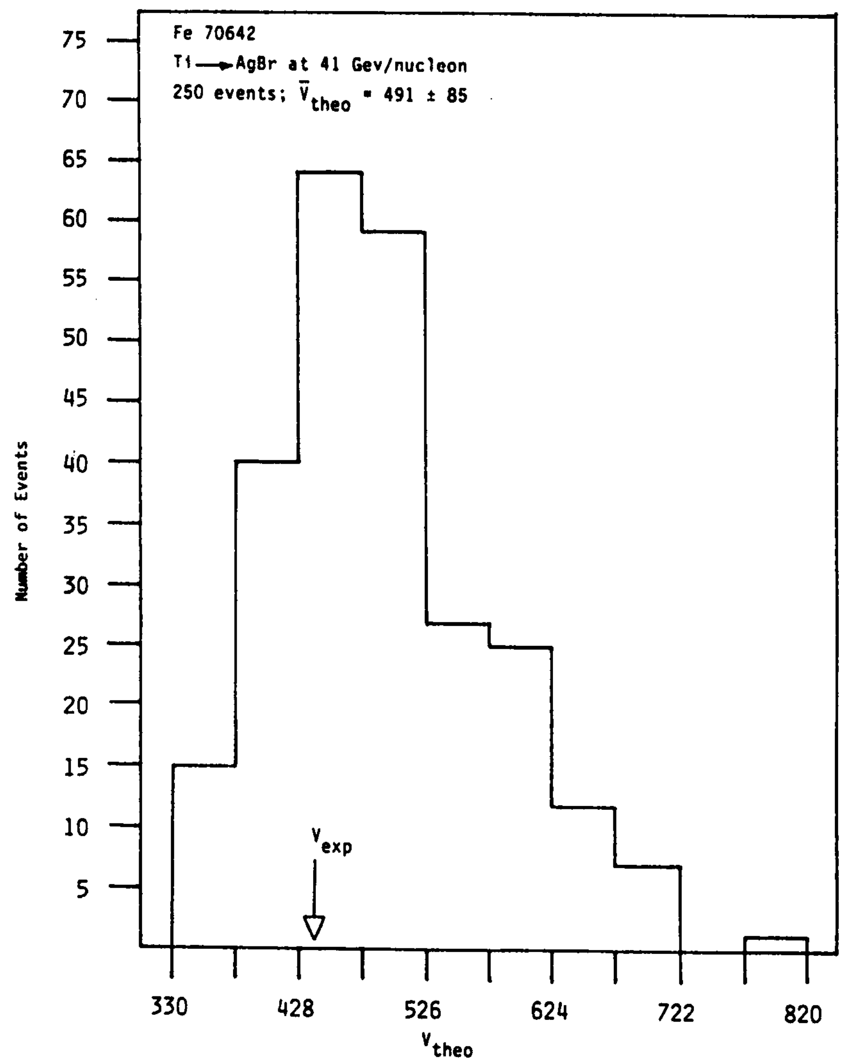

Figure 11. Distribution of the theoretical fluctuations, V_{theo}, for event FE70642.

IV. WOUNDED NUCLEON MODEL SIMULATIONS OF NUCLEUS-NUCLEUS COLLISIONS

In the wounded nucleon model[22] it is assumed that the inelastic collision of two nuclei is an incoherent composition of collisions of individual nucleons and those nucleons that undergo at least one inelastic collision are termed "wounded". The size of the fragment and the number of alpha particles that are emitted in the collision was determined by random sampling of empirical data tables[23]. The remaining mass involved was then divided into wounded and unwounded nucleons. The wounded fraction was found by sampling a distribution which was a binomial approximation with an average value of 0.4. We used this model to simulate events FE6869B and FE70642 and test the azimuthal angular distributions to see how many possessed $(1 - P_{\chi})$ values as large as or larger than the experimental values. Both events were simulated 100 times. In each case a relatively small fraction, ~13%, of the simulated angular distributions had $(1 - P_{\chi})$ values satisfying this condition.

V. SUMMARY AND CONCLUSIONS

The experimental investigation of heavy nuclei collisions at high energies is necessary for establishing to what extent collective phenomena are important in nuclear collisions and to identify those aspects of elementary collisions that get amplified in the nuclear interactions. The methods presented in this paper enable one to place on a quantitative basis the decision as to whether distributions of particles emitted in a collision exhibit nonrandom structure and to characterize the structure in terms of its periodic behavior. In particular, we have seen that discrete Fourier transform analysis is quite effective at the latter. We also find that the present data set supports the assumptions upon which our statistical analyses are based.

One event, Fe---->O at 55 GeV/nucleon shows an azimuthal distribution with a bimodal character describable in terms of a two-component Fourier representation. Results of computer simulations, based on the wounded nucleon picture of the collision, are consistent with the large deviation from uniformity observed in the distribution for this event. However, we do not observe evidences of non-statistical fluctuations in the pseudorapidity distribution for this or other events in the data set.

In order to take on physical meaning the results of these statistical analyses must be combined with deterministic modelling based upon the mechanisms in effect during collision. In this regard, it is important to extend the present activity to include a hydrodynamical description of the collision that takes account of a high energy density and small nuclear radius. This work is presently in progress.

REFERENCES

1. J. Rafelski and M. Danos, NBS Report No. NBSIR 83-2725, June 1983(unpublished).

2. Austin, R. W., et al., Papers at the 18th ICRC, T2-15, (1983).

3. H. A. Gustafsson et al., Phys. Rev. Lett.,52, 1590(1984). and G. Buchwald et al., Phys. Rev. Lett.,52,1594(1984).

4. L. P. Csernai, P. Freier, J. Mevissen, H. Nguyen and L. Waters, Phys. Rev. C., 34,No. 4, 1270(1986).

5. J. Cugnon, Quark Matter '84, proceedings of the Fourth International Conference,Helsinki,1984,K. Kajantie(ed.), p. 101.

6. G. Baym, Quark Matter '84, proceedings of the Fourth International Conference, Helsinki,1984, K. Kajantie(ed.), p. 39.

7. J. Bogdanowicz et al., Nucl. Phys., 40, 270(1963).

8. Lord Rayleigh, Phil. Mag.,10(1880)75;reprinted in Scientific Papers by J. W. Strutt, Baron Rayleigh, 1899, vol. 1, p. 491.

9. F. Cerulus, Approximations to random flight functions in one, two and three dimensions, CERN. 1961.

10. F. Takagi, Phys. Rev. Lett.,53,No. 5 ,427(1984).

11. T. H. Burnett, et al., Proc. 19th ICRC, vol. 6 (August 1985), p. 160.

12. O. Miyamura and T. Tabuki, ICR-Report-128-85-9,July 1985.

13. S. Chandrasekhar, Rev. Mod. Phys. 15 (1943) p. 1.

14. W. T. Eadie, D. Drijard, F. E. James, M. Roos and B. Sadoulet, Statistical Methods in Experimental Physics, North Holland, Amsterdam, 1971,pp.255-262.

15. P. R. Bevington, Data Reduction and Error Analysis for the Physical Sciences, McGraw-Hill Co., New York, 1969, pp. 187-203.

16. R. Ramirez,The FFT-Fundamentals and Concepts,Prentice-Hall, Inc., Englewood Cliffs, N.J., 1985, pp.63-75.

REFERENCES cont.

17. H. J. Weaver, Applications of Discrete and Continuous Fourier Analysis, John Wiley & Sons, New York, N.Y., 1983, pp. 89-109.

18. S. C. McGuire et al., "Azimuthal Anisotropy in Relativistic Nucleus-Nucleus Collisions," Bulletin of the American Physical Society, Vol. 31, No. 1, January 1986, p.57.

19. Fujio Takagi, Tohoku University Report No. TU/85/,July 1985.

20. Milton Abramowitz and Irene A. Stegun, Handbook of Mathematical Functions with Formulas, Graphs and Mathematical Tables, NBS/APS No. 55, Nov. 1970, p. 795.

21. Steven E. Koonin, Computational Physics, The Benjamin/Cummings Publishing Company, Inc., Menlo Park, CA, 1986, pp. 193-194.

22. A. Bialas, M. Bleszynski and W. Czyz, Nuclear Physics B 111, (1976),pp. 461-476.

23. Private Communication with F. E. Roberts.

APPENDIX A

DISCRETE FOURIER TRANSFORM RESULTS

AMPLITUDE DETECTION THRESHOLD (95 PERCENT CONFIDENCE) = .47372770E+01
NOMINAL ONE SIGMA ERROR FOR DETECTED AMPLITUDES = .14869220E+01
(AMPLITUDE FOR K = 0 IS EQUAL TO .17687500E+02)

K	AMPLITUDE	P	PHASE	ERROR	ERROR EST.
1	.22364620E+01	.32266520E+00	-.18415440E+01	.57927700E+00	.66485480E+00
2	.23891970E+01	.27501910E+00	.59778430E+00	.53714970E+00	.62235220E+00
3	.25605320E+01	.22702330E+00	.28142160E+01	.49587720E+00	.58070830E+00
4	.13287680E+01	.67079400E+00	.85196630E+00	.10056050E+01	.11190230E+01
5	.19510240E+01	.42281000E+00	-.87689240E+00	.67509530E+00	.76212420E+00
6	.38256360E+01	.36523770E-01	-.24616610E+01	.31099770E+00	.38867320E+00
7	.56826140E+00	.92957470E+00	.19780410E+01	.16952300E+01	.26166160E+01
8	.24375000E+01	.26089440E+00	.00000000E+00	.52492060E+00	.61001940E+00

COMPLETE DISCRETE FOURIER TRANSFORM RESULTS FOR THE AZIMUTHAL PARTICLE DISTRIBUTION FOR EVENT FE70642. THE QUANTITY P IS THE PROBABILITY FOR RANDOM OCCURRENCE OF A PARTICULAR AMPLITUDE.

AMPLITUDE DETECTION THRESHOLD (95 PERCENT CONFIDENCE) = .32353590E+01

NOMINAL ONE SIGMA ERROR FOR DETECTED AMPLITUDES = .10155050E+01

(AMPLITUDE FOR K = 0 IS EQUAL TO .82500000E+01)

K	AMPLITUDE	P	PHASE	ERROR	ERROR EST.
1	.27174140E+01	.27867770E-01	.12783780E+01	.29747860E+00	.37370270E+00
2	.32430270E+01	.61012520E-02	-.22269760E+01	.24507360E+00	.31313480E+00
3	.83912710E+00	.71077560E+00	.14945810E+01	.10813000E+01	.12101920E+01
4	.17677670E+01	.21977490E+00	.14288990E+01	.48968980E+00	.57445630E+00
5	.10796580E+01	.56826390E+00	.29120080E+01	.84588060E+00	.94058000E+00
6	.18324220E+01	.19631970E+00	-.23376330E+01	.46965910E+00	.55418710E+00
7	.70417740E+00	.78629770E+00	.15718090E-01	.12517890E+01	.14421150E+01
8	.25000000E+00	.97015150E+00	.00000000E+00	.18686320E+01	.40620190E+01

COMPLETE DISCRETE FOURIER TRANSFORM RESULTS FOR THE AZIMUTHAL PARTICLE DISTRIBUTION FOR EVENT FE6869B. THE QUANTITY P IS THE PROBABILITY FOR RANDOM OCCURRENCE OF A PARTICULAR AMPLITUDE.

AMPLITUDE DETECTION THRESHOLD (95 PERCENT CONFIDENCE) = .36172400E+01

NOMINAL ONE SIGMA ERROR FOR DETECTED AMPLITUDES = .11353690E+01

(AMPLITUDE FOR K = 0 IS EQUAL TO .10312500E+02)

K	AMPLITUDE	P	PHASE	ERROR	ERROR EST.
1	.25138080E+01	.86199070E-01	.80489980E+00	.36981080E+00	.45165290E+00
2	.66415410E+00	.84274260E+00	.69786950E+00	.14063860E+01	.17094960E+01
3	.15348990E+01	.40099360E+00	-.16296590E+01	.65312190E+00	.73970250E+00
4	.62500000E+00	.85940480E+00	.22142970E+01	.14567490E+01	.18165900E+01
5	.79033940E+00	.78483380E+00	-.27176190E+01	.12481030E+01	.14365580E+01
6	.12610110E+01	.53967650E+00	-.30834930E+01	.80817000E+00	.90036370E+00
7	.20646360E+01	.19139440E+00	.17815270E+01	.46544180E+00	.54991240E+00
8	.68750000E+00	.83249060E+00	.31415930E+01	.13764760E+01	.16514450E+01

Complete discrete Fourier transform results for the azimuthal particle distribution for event FE61927. The quantity P is the probability for random occurrence of a particular amplitude.

1. REPORT NO. NASA CR-4054	2. GOVERNMENT ACCESSION NO.	3. RECIPIENT'S CATALOG NO.
4. TITLE AND SUBTITLE Statistical Analysis of Secondary Particle Distributions in Relativistic Nucleus-Nucleus Collisions		5. REPORT DATE MARCH 1987 6. PERFORMING ORGANIZATION CODE
7. AUTHOR(S) Stephen C. McGuire		8. PERFORMING ORGANIZATION REPORT #
9. PERFORMING ORGANIZATION NAME AND ADDRESS Department of Physics Alabama A&M University Normal, AL 35762		10. WORK UNIT NO. M-552 11. CONTRACT OR GRANT NO. NAG8-027
12. SPONSORING AGENCY NAME AND ADDRESS National Aeronautics and Space Administration Washington, D.C. 20546		13. TYPE OF REPORT & PERIOD COVERED Contractor Report 14. SPONSORING AGENCY CODE

15. SUPPLEMENTARY NOTES

Marshall Contracting Officer's Representative: Thomas A. Parnell
Marshall Space Flight Center, Space Science Laboratory

16. ABSTRACT

In this paper, we report on our use of several statistical techniques to characterize structure in the angular distributions of secondary particles from nucleus-nucleus collisions in the energy range 24-61 GeV/nucleon. The objective of this work has been to determine whether there are correlations between emitted particle intensity and angle that may be used to support the existence of the quark gluon plasma. The techniques include chi-square null hypothesis tests, the method of discrete Fourier transform analysis, and fluctuation analysis. We have also used the method of composite unit vectors to test for azimuthal asymmetry in a data set of 63 JACEE-3 events. Each method is presented in a manner that provides the reader with some practical detail regarding its application. Of those events with relatively high statistics, Fe--->0 at 55 GeV/nucleon was found to possess an azimuthal distribution with a highly non-random structure. No evidence of non-statistical fluctuations was found in the pseudo-rapidity distributions of the events studied. It is seen that the most effective application of these methods relies upon the availability of many events or single events that possess very high multiplicities.

17. KEY WORDS Heavy Ion-Induced Reactions and Scattering Hadron-Incuded High- and Super-High Energy Interactions, Energy >10 GeV	18. DISTRIBUTION STATEMENT Unclassified - Unlimited Subject Category 73

19. SECURITY CLASSIF. (of this report)	20. SECURITY CLASSIF. (of this page)	21. NO. OF PAGES	22. PRICE
Unclassified	Unclassified	45	A03

For sale by National Technical Information Service, Springfield, Virginia 22161

NASA-Langley, 1987